

Published in final edited form as:

Brain Res. 2008 January 29; 1191: 1. doi:10.1016/j.brainres.2007.10.062.

## Genomic and proteomic analysis of the effects of cannabinoids on normal human astrocytes

B. Bindukumar<sup>a</sup>, S.D. Mahajan<sup>a</sup>, J.L. Reynolds<sup>a</sup>, Z. Hu<sup>b</sup>, D.E. Sykes<sup>a</sup>, R. Aalinkeel<sup>a</sup>, and S.A. Schwartz<sup>a,\*</sup>

<sup>a</sup> Department of Medicine, Division of Allergy, Immunology, and Rheumatology, Buffalo General Hospital, University at Buffalo, State University of NY, Kaleida Health, 100 High Street, Buffalo, NY 14203, USA

<sup>b</sup> Center for Computational Research, Department of Biostatistics, University at Buffalo, State University of NY, Buffalo, NY 14260, USA

### Abstract

Delta-9-tetrahydrocannabinol ( $\Delta^9$ -THC), the main psychoactive component of marijuana, is known to dysregulate various immune responses. Cannabinoid (CB)-1 and -2 receptors are expressed mainly on cells of the central nervous system (CNS) and the immune system. The CNS is the primary target of cannabinoids and astrocytes are known to play a role in various immune responses. Thus we undertook this investigation to determine the global molecular effects of cannabinoids on normal human astrocytes (NHA) using genomic and proteomic analyses. NHA were treated with  $\Delta^9$ -THC and assayed using gene microarrays and two-dimensional (2D) difference gel electrophoresis (DIGE) coupled with mass spectrometry (MS) to elucidate their genomic and proteomic profiles respectively. Our results show that the expression of more than 20 translated protein gene products from NHA was differentially dysregulated by treatment with  $\Delta^9$ -THC compared to untreated, control NHA.

### Keywords

AIDS; Astrocyte; Cannabinoid; Genomic; HIV; Mass spectrometry; Microarray; Proteomic

## 1. Introduction

Marijuana is the most frequently used illegal drug in the US. According to the 2005 National Survey on Drug Use and Health (NSDUH), an estimated 97.5 million Americans aged 12 and older tried marijuana at least once in their lifetime, representing 40.1% of the US population in that age group (Substance Abuse and Mental Health Services Administration, National Survey on Drug Use and Health: National Findings, September 2006). Adverse health events associated with the recreational drug use of marijuana increase dramatically among HIV-1 infected patients. Marijuana is known to increase the risk of a variety of bacterial, fungal, and viral (particularly Herpesvirus) infections. Acquisition of other infections by HIV infected patients can enhance the progression of the underlying HIV infection with a concomitant further loss of CD4<sup>+</sup> T lymphocytes.

Marijuana is a mixture of dried, shredded leaves, stems, seeds, and flowers of the hemp plant (*Cannabis sativa*). Cannabis is a term often used to refer to marijuana and drugs derived from the same plant. The main psychoactive chemical in marijuana is  $\Delta^9$ -tetrahydrocannabinol

\*Corresponding author. Fax: +1 716 859 2999. sasimmun@buffalo.edu (S.A. Schwartz).

(THC). Short-term effects of marijuana use include adverse effects on memory and learning, distorted perception, difficulty with thinking and problem solving, loss of coordination, increased heart rate, and anxiety. THC comprises several chemical structures and metabolites. The  $\Delta^8$ - and  $\Delta^9$ -THC content of certain varieties of marijuana may be as high as 10%. Metabolism of  $\Delta^8$ -THC yields two psychoactive metabolites, 7-hydroxy- $\Delta^8$ -THC and subsequently 7-oxo- $\Delta^8$ -THC.

Marijuana targets the hippocampus, amygdala, and cerebral cortex of the brain due to the presence of cannabinoid receptors in these regions, causing significant cognitive impairment. Cannabinoids also manifest both immunosuppressive and anti-inflammatory properties. The effects of  $\Delta^8$ -THC on the CNS are mediated by the CB-1 cannabinoid receptor that belongs to the family of G-protein-coupled, seven-transmembrane domain proteins (Gerard and Gerard, 1991; Matsuda et al., 1990). Considerable experimental evidence suggests that substances of abuse, such as opiates (Eisenstein et al., 2001) and marijuana (Klein et al., 1998), can impair the immune system and opiates can enhance HIV-1 expression in vitro (Li et al., 2002; Peterson et al., 1990).

In the context of HIV-1 disease, conflicting data exist in the literature that supports both protective and degenerative effects of cannabinoids on the CNS. The synthetic cannabinoid, WIN55,212-2, was found to inhibit HIV-1 expression in a concentration- and time-dependent manner (Peterson et al., 2004). Cannabidiol and THC also were shown to prevent hydroperoxide-induced oxidative damage as well as or better than other antioxidants in a chemical system (Fenton reaction) with neuronal cultures (Hampson et al., 1998). Cannabidiol was more protective against glutamate-induced neurotoxicity than either ascorbate or  $\alpha$ -tocopherol, demonstrating that it is a potent antioxidant (Hampson et al., 1998). Some data indicate that cannabidiol is nontoxic, even when administered to humans chronically or given in large, acute doses of 700 mg/day (Cunha et al., 1980). Smoked and orally administered cannabinoids seemed to be safe for patients with HIV-1 infections, irrespective of their HIV RNA levels, CD4<sup>+</sup> and CD8<sup>+</sup> lymphocytes counts, or protease inhibitor levels, over a 21 day treatment period (Abrams et al., 2003). In an in vivo model of neurodegeneration using neonatal rats, it was shown that  $\Delta^9$ -THC reduced neuronal damage via a CB-1 receptor-mediated mechanism (van der Stelt et al., 2001). Our previous data demonstrate that various drugs of abuse act as cofactors in the pathogenesis of HIV-1 infections (Mahajan et al., 2005, 2006). Given the conflicting nature of various reports in the literature on the effects of cannabinoids on the progression of HIV-1 infections, we undertook a genomic and proteomic analysis to identify the genes and proteins whose expression was significantly modulated by treatment of NHA with  $\Delta^9$ -THC. As we have reported for other drugs of abuse (Mahajan et al., 2002, 2005), we propose that cannabinoids also are cofactors in the pathogenesis of HIV-1 infections by modulating the expression of critical, immunoregulatory genes and proteins, subsequently predisposing to the development of neuroAIDS. In this investigation, we determined the effects of  $\Delta^9$ -THC on the genomic and proteomic profiles of NHA by microarray and DIGE analyses, respectively. Using these technologies, we identified a group of biologically relevant genes and proteins of NHA whose expression was significantly regulated by treatment with cannabinoids. These genes and proteins are associated with inflammation, the immune response, signal transduction, transcriptional regulation, apoptosis, and cell cycle regulation. Strong concordance was observed between our genomic and proteomic results. This study identifies unique biomarkers of HIV-1 infection that are modulated by cannabinoids and may elucidate their role in viral persistence and neuropathogenesis.

## 2. Results

### 2.1. Genomic analysis

To investigate the effect of treatment of NHA with  $10^{-7}$  M  $\Delta^9$ -THC on gene transcription, we compared relative gene expression levels of treated and untreated NHA using microarray analysis. A two-step statistical data analysis was performed. First, the paired *t*-test (Baldi and Long, 2001) was used to detect differentially expressed genes, resulting in the identification of 478 significantly ( $p < 0.05$ ), differentially expressed genes. Fig. 1 is the scatter plot of the average  $\log_2$  ratio between normal and treated samples for 3998 genes. Statistically significant ( $p < 0.05$ ) differences in the expression of genes identified by two-step analysis of *t*-test and Significance Analysis of Microarrays (SAM) (Tusher et al., 2001) are shown as black asterisks (\*). All 478 differentially expressed genes were up-regulated. While some genes were down-regulated, none reached statistical significance.

A gene ontology analysis of our complete data set of reproducibly changed genes using GeneSifter™ software allowed us to classify them into functional groups according to their role in biological processes or molecular functions relevant to immunomodulatory effects (Table 1). Table 2 lists specific, differentially expressed ( $p < 0.05$ ) genes according to their physiological roles. We observed that a number of genes involved in important cellular functions were differentially regulated upon treatment of NHA with  $\Delta^9$ -THC.

### 2.2. Effect of $\Delta^9$ -THC treatment of NHA on the expression of specific genes as measured by real-time, quantitative polymerase chain reaction (Q PCR)

To verify the effect of  $\Delta^9$ -THC on mRNA expression by the modulated genes, we selected a representative few and quantitated the relative mRNA expression of the  $\Delta^9$ -THC treated and untreated NHA by Q PCR. Results are shown in Fig. 2. Genes demonstrating the greatest up-regulation of expression by Q PCR included brain creatine kinase (2.45 fold-increase,  $p < 0.001$ ); heat shock protein (HSP) 60 (1.76 fold-increase  $p < 0.001$ ); aldolase A (1.65 fold-increase,  $p < 0.001$ ); and glutathione peroxidase (1.53 fold-increase  $p < 0.001$ ). Other genes up-regulated on THC treatment are cystatin B (1.3 fold-increase,  $p = 0.018$ ); cathepsin D (1.41 fold-increase,  $p = 0.011$ ); lysophospholipase 2 (1.24 fold-increase,  $p = 0.021$ ); and heterogeneous nuclear ribonucleoprotein F (1.17 fold-increase,  $p = 0.035$ ). The Q PCR results agree with the proteomic data below except for the enolase gene where the change in expression was not significant with Q PCR.

### 2.3. Proteomic analysis

The effects of  $\Delta^9$ -THC on NHA were examined utilizing 2D-DIGE technology. Protein expression was compared between untreated NHA and NHA treated with  $10^{-7}$  M  $\Delta^9$ -THC for 48 h. A mixed sample containing an equal amount of protein extract from all individual samples was included as an internal standard. After 2D gel electrophoresis, the Cy2, Cy3, and Cy5 dye stained images from the THC treated NHA in comparison with the untreated NHA controls were evaluated with the biological variation analysis (BVA) module of the DeCyder™ software used to analyze 2D-DIGE. This revealed statistically significant (Student's *t*-test  $p < 0.05$ ) changes in the abundance of 31 different proteins, as measured by spot volume ratios. Twenty-four spots were selected in the order of the significance of their respective volume ratios for further analysis by nano high performance liquid chromatography followed by tandem mass spectrometry (LC-MS/MS). Proteins from 16 gel spots were successfully identified. Fig. 3 is the SYPRO-Ruby dye stained 2D gel showing all protein spots. The differentially expressed, significantly up-regulated spots which were selected for protein identification are identified by numbered outlines in Fig. 3. Multiple proteins were identified in some spots. Presently there is no way to separate different proteins with identical molecular weights and isoelectric point (*pI*) values using this technology. The list of identified proteins is presented in Table 3.

Expression of all identified proteins was significantly up-regulated by treatment of NHA with  $\Delta^9$ -THC. Up-regulation of glutathione peroxidase (GPX) was greatest among the identified proteins (12.2 fold-increase,  $p=0.013$ ). Fig. 4 shows the 2D gel pattern of proteins from untreated, control NHA (Fig. 4A) and NHA treated with  $10^{-7}$  M  $\Delta^9$ -THC (Fig. 4B). The spot intensities are compared for untreated NHA (Fig. 4C) and  $\Delta^9$ -THC treated NHA (Fig. 4D). Peptide extracts of the digested protein spots after HPLC were directed into a ThermoFinnigan LCQ Deca XP Plus ion trap, mass spectrometer yielding the mass of the fragments. The mass range scanned was 0–1500 amu. Fig. 4E shows the MS/MS spectra of fragment ions from representative tryptic peptides, LAAAAAAQSVYAFSAR and PLAGGEPVSLGSLR, obtained from spot # 3027 which was subsequently identified as glutathione peroxidase. The  $x$  axis is the mass to charge ratio and the  $y$  axis is the relative abundance. These peptides, LAAAAAAQSVYAFSAR and PLAGGEPVSLGSLR, produced strong fragment ions with molecular mass 714.3 Da and 828.4 Da, respectively, which strongly matched with the spectra used as the empirical comparators. From such data, specific proteins can be identified. Other significantly up-regulated proteins include nuclear ribonucleoprotein F/cathepsin D (3.8 fold-increase,  $p=0.0053$ ) and putative elongation factor Tu/HSP60 (2.0 fold-increase,  $p=0.038$ ). A list of analyzed spots arranged on the basis of the significance ( $p$  value) of their fold-increase in response to treatment of NHA with  $\Delta^9$ -THC is shown in Fig. 3.

#### 2.4. Glutathione peroxidase activity assay

To confirm the effect of  $\Delta^9$ -THC treatment of NHA on the up-regulation of GPX protein expression, cellular GPX enzyme activity also was measured. GPX activity was significantly enhanced on treatment of NHA with  $\Delta^9$ -THC (Fig. 5). The activity measured for the  $\Delta^9$ -THC treated NHA ( $44.9 \pm 1.59$  units/min/mg protein) was significantly ( $p < 0.001$ ) higher than the untreated control ( $37.7 \pm 1.03$  units/min/mg protein).

### 3. Discussion

Cannabinoids have anti-inflammatory and neuroprotective effects on the brain but the mechanisms underlying these actions are unclear. We have shown that  $\Delta^9$ -THC, the principal psychoactive component of *C. sativa*, significantly modulates the expression of a host of biologically relevant genes and their translated protein products in NHA using genomic and proteomic analyses. It is interesting to note that treatment of NHA with  $10^{-7}$  M  $\Delta^9$ -THC for 48 h in general significantly increased the expression of numerous genes and proteins. While the expression of some genes and proteins was down-regulated, this effect was not statistically significant. Twenty-four up-regulated proteins were identified by LC-MS/MS and categorized according to their biological functions such as glycolysis, binding and folding, kinase, and molecular chaperone activities by gene ontology analysis. Table 2 shows details of these identified proteins.

As stated in the Results section, our entire data set consisted of 5043 genes that were analyzed using data standardization, image acquisition and analysis, normalization, exploratory data analysis, statistical significance inference, gene function classification, and finally speculation on the pathways involved. Fig. 1 shows the genes that were significantly up-regulated in  $\Delta^9$ -THC treated NHA in comparison with untreated, control NHA. Table 1 lists significantly up-regulated genes categorized on the basis of their molecular functions and cellular processes. Our results demonstrate that cannabinoids modulate numerous genes that play key biological roles, including regulation of the ubiquitin pathway, signal transduction, transcription, the cell cycle, and glucose metabolism.

We have already proposed that various up-regulated genes and their protein products play a role in the neuropathogenesis of HIV-1 infections. GPX expression was up-regulated by 12.2-fold, more than any other protein. GPX is an anti-oxidant that scavenges free radicals. There

are reports that GPX is substantially reduced during HIV-1 infection causing oxidative stress (Ogunro et al., 2006; Price et al., 2005). Overexpression of GPX using a Herpes vector eliminated the neurotoxicity induced by HIV-1 protein, gp120 (Brooke et al., 2002). These results suggest that cannabinoids may ameliorate neurotoxic effects associated with HIV-1 infections.

Another protein up-regulated by treatment of NHA with  $\Delta^9$ -THC is brain creatine kinase (CK). Both creatine and phosphocreatine serve in brain energy metabolism in association with the activity of creatine kinase (CK) (Ames, 2000). Phosphocreatine may provide a buffer for rapid, transient increases in energy demand due to the onset of neuronal firing (Smith et al., 2002). The presence of brain type B CK in Bergmann glial cells and astrocytes is very likely related to the energy requirements for ion homeostasis in the brain, as well as for metabolite and neurotransmitter trafficking between glial cells and neurons. CK and its substrates, creatine and phosphocreatine, constitute an intricate cellular energy buffering and transport system connecting sites of energy production (mitochondria) with sites of energy consumption (Hemmer and Wallimann, 1993). Creatine stabilizes mitochondrial CK and inhibits opening of the mitochondrial transition pore (O'Gorman et al., 1996). Creatine administration to G93A transgenic mice protected them from increases in biochemical indices of oxidative damage (Klivenyi et al., 1999).

HSP-60 is a stress protein associated with protein folding and hence supports cell survival (Lindquist and Craig, 1988). Exposure of neurons to elevated temperature is sufficient to induce the heat shock response and to provide neuroprotection (Mailhos et al., 1993). The major role of HSP-60 is its involvement in the folding of proteins during mitochondrial import. Once properly folded, the protein is unable to be a target for binding to HSP-60 (Langer et al., 1992). Interestingly, it has been reported that HSP-60 interacts with gp41, a transmembrane protein anchoring the surface protein gp120 to the envelope of HIV-1. In addition, gp41 mediates fusion between the membranes of the virus, HIV-1, and the host cell, a step essential for viral entry (Speth et al., 1999). In the current study, HSP60 was found to be overexpressed upon treatment of NHA with  $\Delta^9$ -THC.

Aldolase A and enolase 1 are additional proteins that were up-regulated by  $\Delta^9$ -THC treatment of NHA. It has been shown that aldolase A and enolase 1 are transcribed in response to hypoxia (Semenza et al., 1996). Another protein up-regulated on treatment of NHA with  $\Delta^9$ -THC is cystatin B, important in maintaining normal neuronal architecture and size (Shannon et al., 2002). Brains of cystatin B deficient, adult mice are smaller than normal controls, and this size difference is paralleled by low body weight, a greater density of neurons in the cerebellar granular cell layer, as well as an increased susceptibility of granule cells to undergo apoptosis (Lieuallen et al., 2001). In humans, advanced neurodegenerative syndromes are often accompanied by severe wasting (Beyer et al., 1995; Grundman et al., 1996), a finding that correlates with both the degree and type of neurological impairment. This observation is particularly relevant to infections with HIV-1 which, in an advanced state, is associated with neurodegeneration and a wasting syndrome.

While the immunosuppressive effects of cannabinoids (Cabral and Vasquez, 1992; Morahan et al., 1979) and their modulatory activities on immune cell functions (Cabral and Mishkin, 1989; Fischer-Stenger et al., 1992; Klein et al., 1991) have been reported previously, there is recent evidence supporting the premise that cannabinoids also have anti-inflammatory (Pryce et al., 2003), neuroprotective (Shen and Thayer, 1998), and anti-tumor properties (Galve-Roperh et al., 2000). Cannabinoids have been shown to be neuroprotective in a variety of in vitro and in vivo models of neuronal excitotoxicity (van der Stelt and Di Marzo, 2005; McCarty, 2006).



Marijuana and other exogenous cannabinoids alter immune functions and decrease host resistance to infections in vitro and in experimental animals. The mechanism by which  $\Delta^9$ -THC and other cannabinoids affect immune responses may be via the cannabinoid receptors, CB-1 and CB-2. Endogenous cannabinoids or endocannabinoids have been identified and have also been proposed to modulate immune functions through cannabinoid receptors on cells of the immune system. Exogenous cannabinoids may disturb a homeostatic balance between endocannabinoids and the immune system. This may occur by perturbing the balance between T helper (Th)1 pro-inflammatory versus Th2 anti-inflammatory cytokines. Cannabinoids, by virtue of their immunomodulatory properties, have the potential to serve as therapeutic agents for altered immune states (e.g. autoimmune diseases). It is further speculated that modulation of the gene and protein expression of several key physiological regulators in the brain by cannabinoids, resulting in neuroprotective effects, also may be due to alterations in the balance between pro-inflammatory and anti-inflammatory cytokines (Table 2). We are currently undertaking further studies to assess these possibilities.

## 4. Experimental procedures

### 4.1. Cell culture

Primary NHA were obtained from Cell Systems (Kirkland, WA). NHA ( $1 \times 10^6$ /ml) were cultured overnight in 6 well plates using Astrocyte Basal Medium (Cell Systems) with 10% serum and then treated with or without  $\Delta^9$ -THC (Sigma-Aldrich, St. Louis MO) at a concentration of  $1 \times 10^{-7}$  M for 48 h; time and concentration used were based on earlier studies (Brenneisen et al., 1996).

### 4.2. Protein extraction

After treatment, NHA were washed twice with  $1 \times$  PBS (Invitrogen, Grand Island, NY). Total protein was extracted using standard cell lysis buffer (30 mM Tris-Cl; 8 M urea; 4% (w/v) CHAPS, adjusted to pH 8.5) for 10 min on ice. The cell lysate was centrifuged at  $4^\circ\text{C}$  for 10 min at  $12,000 \times g$  and was further purified by precipitation with chloroform/methanol as described (Wessel and Flugge, 1984). Samples were resuspended in standard cell lysis buffer. Protein concentrations were determined using the Coomassie Protein Reagent (Bio-Rad, Hercules CA) prior to DIGE analysis.

### 4.3. Two-dimensional differential in-gel electrophoresis (2-D DIGE)

Proteomics research technologies are rapidly changing our understanding of complex and dynamic biological systems by providing information relevant to functionally associated changes in protein abundances, protein-protein interactions, and post-translational modifications (Aebersold et al., 2000; Harry et al., 2000; Pandey and Mann, 2000; Tonella et al., 1998). Two-dimensional gel electrophoresis can simultaneously separate and display hundreds to thousands of different proteins. This method separates proteins in 2 dimensions according to their isoelectric point and their molecular size. Fluorescent, 2-D DIGE (Tonge et al., 2001; Unlu et al., 1997; Zhou et al., 2002) allows the multiplex analysis of 3 sample proteomes on the same gel. The Ettan DIGE technique developed by GE Healthcare (Piscataway, NJ, USA) was used to detect differences in protein abundance between untreated and experimental samples. The Ettan DIGE system uses 3 CyDye DIGE fluors (Cy2, Cy3, Cy5), each with a unique fluorescent wavelength, matched for mass and charge. CyDyes form a covalent bond with the free epsilon amino group on lysine residues of the sample proteins. CyDyes label approximately 2% of the lysine residues. This system allows for 2 experimental samples and an internal standard to be simultaneously separated on the same gel. The internal standard comprised a pool of an equal amount of all the experimental samples. The use of an internal standard facilitates accurate inter-gel matching of spots, and allows for data normalization between gels to minimize gel to gel experimental variability (Tonge et al.,

2001). Cell lysates were labeled with CyDye per the manufacturer. All reagents used were from GE Healthcare (Amersham Biosciences, Piscataway, NJ). Briefly, 50  $\mu\text{g}$  of cell lysate was labeled with 400 pmol of either Cy3 or Cy5 or Cy2 (Cy2 was used to label the internal standard), kept on ice for 30 min, and then quenched with a 50 fold molar excess of free lysine. Cy3, Cy5, and Cy2 labeled samples and unlabelled protein (500–800  $\mu\text{g}$ ) were pooled. An equal volume of 2 $\times$  sample buffer (8 M urea; 2% (v/v) Pharmalytes 3–10; 2% (w/v) dithiothreitol (DTT); 4% (w/v) CHAPS) was added and incubated on ice for 10 min. The total volume of sample was adjusted to 450  $\mu\text{l}$  with rehydration buffer (4% (w/v) CHAPS; 8 M urea; 1% (v/v) Pharmalytes 3–10 nonlinear (NL); 13 mM DTT). Samples were applied to immobilized pH gradient (IPG) strips (24 cm, pH 3–10 non-linear), and absorbed by active rehydration at 30 V for 13 h. Isoelectric focusing was carried out using an IPGphor IEF system with a 3 phase program; first phase at 500 V for 1 h, second phase at 1000 V for 1 h, and third phase (linear gradient) 8000 V to 64000 V for 2 h (50  $\mu\text{A}$  maximum per strip). Prior to separation in the second dimension, strips were equilibrated for 15 min in equilibration buffer I (50 mM Tris–HCl, 6 M urea, 30% (v/v) glycerol, 2% (w/v) SDS, 0.5% (w/v) DTT). The strips were again equilibrated for 15 min in equilibration buffer II (50 mM Tris–HCl, 6 M urea, 30% (v/v) glycerol, 2% (w/v) SDS, 4.5% (w/v) iodoacetamide) and the equilibrated IPG strips were transferred onto 18 $\times$ 20 cm, 12.5% uniform polyacrylamide gels poured between low fluorescence glass plates. Gels were bonded to inner plates using Bind-Silane solution (Promega, Madison, WI) according to the manufacturer. Strips were overlaid with 0.9% agarose in 1 $\times$  running buffer containing bromophenol blue and were run for 16 h (1.8 W/gel overnight) at 15  $^{\circ}\text{C}$  in an Ettan DALT electrophoresis system. After the run was completed, the 2D gels were scanned 3 times with a Typhoon 9410 imager, each time at different excitation wavelengths (Cy3, 532 nm; Cy5, 633 nm; Cy2, 488 nm). Images were cropped with ImageQuant v5.2 software and then imported into DeCyder Differential In-gel Analysis (DIA) v5.0 software from GE Healthcare for spot identification and normalization of spot intensities within each gel.

Gels were fixed in 30% (v/v) methanol, 7.5% (v/v) acetic acid for 3 h, and stained with SYPRO-Ruby dye (Molecular Probes, Eugene, OR) overnight at room temperature. Gels were destained in water and then scanned using the Typhoon 9410 scanner. Spots of interest were excised from the gel using the Ettan Spot Picker. DeCyder software (GE Healthcare) was specifically developed for use with the Ettan DIGE system. DeCyder software allows for automatic detection of spots, background subtraction, quantitation, normalization, internal standardization, and integral matching. The differential in-gel analysis (DIA) component of DeCyder software draws boundaries around spots in a composite gel image obtained from the intra-gel overlap of the Cy2, Cy3, and Cy5 scanned images and normalizes the data from each CyDye to account for differences in dye fluorescence intensity and scanner sensitivity. The abundance difference between samples run on the same gel was then analyzed. The biological variation analysis (BVA) component of DeCyder software was then used to match all image comparisons from in-gel analysis for a cross-gel statistical analysis. DeCyder BVA initially calculates normalized intensities (standard abundance) for all spots by comparison to the internal standard, and from this an average volume ratio and a Student's paired *t*-test derived *p* value were calculated for each spot. A paired *t*-test derived *p* value of  $\leq 0.05$  was considered statistically significant (Tonge et al., 2001).

#### 4.4. Protein identification

Spots excised from the 2D gel were sent to the Proteomic Analysis Laboratory at the University of Arizona for mass spectrometry. In-gel digestion and nano high performance liquid chromatography (HPLC) followed by tandem mass spectrometry (MS/MS) were performed as described (Breci et al., 2005). Briefly, gel slices were destained (Breci et al., 2005; Cooper et al., 2003) and digested with trypsin (Wilm et al., 1996). The tryptic peptides were extracted

with 5% formic acid/50% CH<sub>3</sub>CN. HPLC was performed using a microbore system (Surveyor, Thermo-Finnigan, San Jose, CA). The HPLC column eluate was directed into a ThermoFinnigan LCQ Deca XP Plus ion trap mass spectrometer. Automated peak recognition, dynamic exclusion, and daughter ion scanning of the two most intense ions were performed with the aid of Xcalibur software (Andon et al., 2002; Haynes et al., 1998). Spectra were scanned over the range of 0–1400 mass units. MS/MS data were analyzed using SEQUEST software and searched against the latest version of the National Center for Biotechnology's public nonredundant protein database.

#### 4.5. Glutathione peroxidase (GPX) activity assay

GPX enzyme activity was determined using a spectrophotometric method according to the manufacturer's instructions (ZeptoMetrix, Buffalo, NY). Treated and untreated NHA were homogenized in GPX assay buffer plus 1 mM β-mercaptoethanol. After centrifugation, the supernates were used for the assay per the manufacturer's instructions. Activity was measured as arbitrary units/min/mg of protein.

#### 4.6. RNA extraction and quantitative real-time, quantitative polymerase chain reaction (Q PCR)

Cytoplasmic RNA was extracted by the acid guanidinium thiocyanate–phenol–chloroform (AGPC) method (Chomczynski and Sacchi, 1987). The RNA pellet was dissolved in DEPC water, quantified, checked for integrity using agarose gel electrophoresis, and stored at –70 °C. Q PCR (Bindukumar et al., 2005) was performed with the MX3005P Stratagene sequence detection system using SYBR green reagents according to the manufacturer's instructions (Stratagene). Equal amounts of RNA from NHA treated with Δ<sup>9</sup>-THC and untreated controls were reverse-transcribed into first-strand cDNA and used as PCR templates in reactions to obtain the threshold cycle (Ct). Ct was normalized using the known Ct from the housekeeping gene, β-actin, to obtain ΔCt. To compare the relative levels of gene expression of different genes of interest, ΔΔCt values were calculated using gene expression from the untreated control cells. The ΔΔCt values are representative of the real fold increase in gene expression.

#### 4.7. cDNA microarrays

The arrays used in this experiment were produced at the Roswell Park Cancer Institute (RPCI) Microarray and Genomics Core Facility. Approximately 5043 cDNA clones (Research Genetics) were selected based on their association with the immunological response as cited in the scientific literature. Cloned cDNAs were printed in triplicate using a MicroGridII TAS arrayer and MicroSpot 2500 split pins (Apogent Discoveries, Hudson, NH). Total RNA was extracted from Δ<sup>9</sup>-THC treated NHA and labeled with Cy5 dye (GE Healthcare, Piscataway, NJ) and total RNA from the untreated control NHA was labeled with Cy3 dye (GE Healthcare, Piscataway, NJ). For each reverse transcription reaction, 2.5 μg of RNA was mixed with 2 μl of random primers (Invitrogen, Carlsbad, CA) in a total volume of 10 μl, heated to 70 °C for 5 min, and cooled to 42 °C. An equal volume of reaction mix (4 μl of 5× first-strand buffer, 2 μl of 10× dNTP mix, 2 μl of DTT, 1 μl of deionized H<sub>2</sub>O, and 1 μl of Powerscript reverse transcriptase) was added to this sample according to the manufacturer's instructions. After 1 h incubation at 42 °C, the RNA–cDNA complex was denatured by incubation at 70 °C for 5 min. The mixture was cooled to 37 °C and incubated for 15 min with 0.2 μl of RNase H (10 U/μl). The resultant amino-modified cDNA was purified, precipitated, and fluorescently labeled. Prior to hybridization, the two separate probes were resuspended in 10 μl of distilled H<sub>2</sub>O, combined, and mixed with 2 μl of human Cot1 (20 μg/μl; Invitrogen) and 2 μl of polyA (20 μg/μl; Sigma-Aldrich). The probe mixture was denatured at 95 °C for 5 min, placed on ice for 1 min, and prepared for hybridization by the addition of 110 μl of preheated (65 °C) SlideHyb No. 3 buffer (Ambion, Austin, TX). After 5 min incubation at 65 °C, the probe



solution was placed on the array in an assembled GeneTAC hybridization station module (Genomic Solutions, Inc., Ann Arbor, MI). The slides were incubated overnight at 55 °C for 16 to 18 h with occasional pulsation of the hybridization solution. After hybridization, the slides were spun dry and scanned immediately on an Affymetrix 428 scanner to generate high resolution images for both Cy3 and Cy5 channels. Two hybridizations for each RNA sample were performed, switching the dyes in the second hybridization to account for possible dye bias. The hybridized slides were scanned using an Axon GenePix 4200A Scanner. The background-corrected signal for each cDNA spot is the mean signal (of all the pixels in the region) minus the mean local background. The ratios were then normalized on the log scale across the entire slide. For each clone on the slide, the expression ratio is the mean of all of its replicates on the log scale. The results from the two slides that make up the dye flip were then averaged on the log scale, and this became the final expression ratio of that clone generated along with a spreadsheet detailing expression ratios of all normalized spots.

#### 4.8. Microarray data analysis

Expression data extracted from image files were first checked by an M ( $\log_2(\text{Cy3}/\text{Cy5})$ ) versus A ( $\log_2(\text{Cy3}) + \log_2(\text{Cy5}/2)$ ) plot to see whether intensity-dependent expression bias existed between spots (genes) labeled with Cy3 and Cy5 on each individual slide. After finding that intensity-dependent expression bias did exist for all slides, we first performed a Lowess data normalization to correct the observed intensity-dependent expression bias. We then performed a global normalization to bring the median expression values of Cy3 and Cy5 for all replicates to the same scale. This was done by selecting a baseline array (e.g. Cy3) from one of the slides, followed by scaling expression values of the remaining arrays to the median value of the baseline array ( $\tilde{m}_{\text{base}}$ ):

$$x'_i = \frac{\tilde{m}_{\text{base}}}{\tilde{m}_i} x_i.$$

After data normalization, the average intensity of individual genes from multiple spots on each slide was computed using an in-house developed PERL script. A total of 5043 average expression values were obtained, including empty, dry, null, and DMSO control spots. Paired *t*-tests on normalized intensities with *p* values <0.05 were used to generate a list of genes with significant changes in expression between normal and THC treated samples. The false positive rate of the significant genes was estimated by using the SAM algorithm (Tusher et al., 2001).

Further analysis of microarray data was done using the gene ontology analysis tool of the Genesifter software (VizXlabs, Seattle, WA). The use of gene ontologies enables us to summarize results of quantitative analysis and annotate genes and their products with a limited set of attributes. A gene product has one or more molecular functions and is used in one or more biological processes; it might be associated with one or more cellular components. Molecular function describes activities, such as catalytic or binding effects. In gene ontology, molecular functions represent activities rather than entities (molecules or complexes) that perform the actions and do not specify where or when, or in what context, the action takes place. Molecular functions generally correspond to activities that can be performed by individual gene products, but some activities are performed by complexes of gene products. A cellular process is a series of events accomplished by one or more ordered assemblies of molecular functions. GeneSifter software allows us to do user-defined filtering to focus on data of greatest interest and then these queried files can be exported for secondary analyses. GeneSifter software rapidly characterizes the biology involved in a particular experiment, and helps identify specific genes of interest from a list of potential targets by identification of broad biological themes.

#### 4.9. Quality control

Quality control measures including ratios of the housekeeping genes, glyceraldehyde-3-phosphate dehydrogenase (G3PDH) and  $\beta$ -actin, scaling factors, background, and  $Q$ -values all were within acceptable limits. A comparison analysis was performed for the cannabinoid treated sample against its corresponding untreated control as the baseline; ‘signal’, ‘detection’, ‘signal log ratio’, ‘change’, and ‘change  $p$  value’ were obtained from this analysis. Fold-change was calculated from the signal log ratio. Only transcripts that were present in at least one of the two samples (untreated control or  $\Delta^9$ -THC treated NHA), i.e. intra-experimental and those that were reproducibly changed in the same direction across independent experiments, were analyzed further.

#### Acknowledgments

This work was supported by grants from the Margaret Duffy and Robert Cameron Troup Memorial Fund for Cancer Research of Kaleida Health and the Kaleida Health Foundation.

#### References

- Abrams DI, Hilton JF, Leiser RJ, Shade SB, Elbeik TA, Aweeka FT, Benowitz NL, Bredt BM, Kosel B, Aberg JA, Deeks SG, Mitchell TF, Mulligan K, Bacchetti P, McCune JM, Schambelan M. Short-term effects of cannabinoids in patients with HIV-1 infection: a randomized, placebo-controlled clinical trial. *Ann Intern Med* 2003;139:258–266. [PubMed: 12965981]
- Aebersold R, Rist B, Gygi SP. Quantitative proteome analysis: methods and applications. *Ann NY Acad Sci* 2000;919:33–47. [PubMed: 11083095]
- Ames A III. CNS energy metabolism as related to function. *Brain Res Brain Res Rev* 2000;34:42–68. [PubMed: 11086186]
- Andon NL, Hollingworth S, Koller A, Greenland AJ, Yates JR III, Haynes JR. Proteomic characterization of wheat amyloplasts using identification of proteins by tandem mass spectrometry. *Proteomics* 2002;2:1156–1168. [PubMed: 12362334]
- Baldi P, Long AD. A Bayesian framework for the analysis of microarray expression data: regularized  $t$ -test and statistical inferences of gene changes. *Bioinformatics* 2001;17:509–519. [PubMed: 11395427]
- Beyer PL, Palarino MY, Michalek D, Busenbark K, Koller WC. Weight change and body composition in patients with Parkinson’s disease. *J Am Diet Assoc* 1995;95:979–983. [PubMed: 7657912]
- Bindukumar B, Schwartz SA, Nair MP, Aalinkeel R, Kawinski E, Chadha KC. Prostate-specific antigen modulates the expression of genes involved in prostate tumor growth. *Neoplasia* 2005;7:241–252. [PubMed: 15799824]
- Breci L, Hattrup E, Keeler M, Letarte J, Johnson R, Haynes PA. Comprehensive proteomics in yeast using chromatographic fractionation, gas phase fractionation, protein gel electrophoresis, and isoelectric focusing. *Proteomics* 2005;5:2018–2028. [PubMed: 15852344]
- Brenneisen R, Egli A, Elshohly MA, Henn V, Spiess Y. The effect of orally and rectally administered delta 9-tetrahydrocannabinol on spasticity: a pilot study with 2 patients. *Int J Clin Pharmacol Ther* 1996;34:446–452. [PubMed: 8897084]
- Brooke SM, McLaughlin JR, Cortopassi KM, Sapolsky RM. Effect of GP120 on glutathione peroxidase activity in cortical cultures and the interaction with steroid hormones. *J Neurochem* 2002;81:277–284. [PubMed: 12064474]
- Cabral GA, Mishkin EM. Delta-9-tetrahydrocannabinol inhibits macrophage protein expression in response to bacterial immunomodulators. *J Toxicol Environ Health* 1989;26:175–182. [PubMed: 2537903]
- Cabral GA, Vasquez R. Delta 9-tetrahydrocannabinol suppresses macrophage extrinsic antiherspesvirus activity. *Proc Soc Exp Biol Med* 1992;199:255–263. [PubMed: 1311105]
- Chomczynski P, Sacchi N. Single-step method of RNA isolation by acid guanidinium thiocyanate–phenol–chloroform extraction. *Anal Biochem* 1987;162:156–159. [PubMed: 2440339]

- Cooper B, Eckert D, Andon NL, Yates JR, Haynes PA. Investigative proteomics: identification of an unknown plant virus from infected plants using mass spectrometry. *J Am Soc Mass Spectrom* 2003;14:736–741. [PubMed: 12837595]
- Cunha JM, Carlini EA, Pereira AE, Ramos OL, Pimentel C, Gagliardi R, Sanvito WL, Lander N, Mechoulam R. Chronic administration of cannabidiol to healthy volunteers and epileptic patients. *Pharmacology* 1980;21:175–185. [PubMed: 7413719]
- Eisenstein LK, MacFarland AS, Peng X, Hilburger ME, Rahim RT, Meissler LJ Jr, Rogers TJ, Wan AC, Adler MW. Effect of opioids on oral Salmonella infection and immune function. *Adv Exp Med Biol* 2001;493:169–176. [PubMed: 11727763]
- Fischer-Stenger K, Updegrave AW, Cabral GA. Delta 9-tetrahydrocannabinol decreases cytotoxic T lymphocyte activity to herpes simplex virus type 1-infected cells. *Proc Soc Exp Biol Med* 1992;200:422–430. [PubMed: 1319584]
- Galve-Roperh I, Sanchez C, Cortes ML, del Pulgar TG, Izquierdo M, Guzman M. Anti-tumoral action of cannabinoids: involvement of sustained ceramide accumulation and extracellular signal-regulated kinase activation. *Nat Med* 2000;6:313–319. [PubMed: 10700234]
- Gerard NP, Gerard C. Molecular cloning of the human neurokinin-2 receptor cDNA by polymerase chain reaction and isolation of the gene. *Ann NY Acad Sci* 1991;632:389–390. [PubMed: 1659296]
- Grundman M, Corey-Bloom J, Jernigan T, Archibald S, Thal LJ. Low body weight in Alzheimer's disease is associated with mesial temporal cortex atrophy. *Neurology* 1996;46:1585–1591. [PubMed: 8649553]
- Hampson AJ, Grimaldi M, Axelrod J, Wink D. Cannabidiol and (-)Delta9-tetrahydrocannabinol are neuroprotective antioxidants. *Proc Natl Acad Sci U S A* 1998;95:8268–8273. [PubMed: 9653176]
- Harry JL, Wilkins MR, Herbert BR, Packer NH, Gooley AA, Williams KL. Proteomics: capacity versus utility. *Electrophoresis* 2000;21:1071–1081. [PubMed: 10786881]
- Haynes PA, Gygi SP, Figeys D, Aebersold R. Proteome analysis: biological assay or data archive? *Electrophoresis* 1998;19:1862–1871. [PubMed: 9740046]
- Hemmer W, Wallimann T. Functional aspects of creatine kinase in brain. *Dev Neurosci* 1993;15:249–260. [PubMed: 7805577]
- Klein TW, Kawakami Y, Newton C, Friedman H. Marijuana components suppress induction and cytolytic function of murine cytotoxic T cells in vitro and in vivo. *J Toxicol Environ Health* 1991;32:465–477. [PubMed: 1850002]
- Klein TW, Friedman H, Specter S. Marijuana, immunity and infection. *J Neuroimmunol* 1998;83:102–115. [PubMed: 9610678]
- Klivenyi P, Ferrante RJ, Matthews RT, Bogdanov MB, Klein AM, Andreassen OA, Mueller G, Wermer M, Kaddurah-Daouk R, Beal MF. Neuroprotective effects of creatine in a transgenic animal model of amyotrophic lateral sclerosis. *Nat Med* 1999;5:347–350. [PubMed: 10086395]
- Langer T, Pfeifer G, Martin J, Baumeister W, Hartl FU. Chaperonin-mediated protein folding: GroES binds to one end of the GroEL cylinder, which accommodates the protein substrate within its central cavity. *EMBO J* 1992;11:4757–4765. [PubMed: 1361169]
- Li Y, Wang X, Tian S, Guo CJ, Douglas SD, Ho WZ. Methadone enhances human immunodeficiency virus infection of human immune cells. *J Infect Dis* 2002;185:118–122. [PubMed: 11756991]
- Lieuallen K, Pennacchio LA, Park M, Myers RM, Lennon GG. Cystatin B-deficient mice have increased expression of apoptosis and glial activation genes. *Hum Mol Genet* 2001;10:1867–1871. [PubMed: 11555622]
- Lindquist S, Craig EA. The heat-shock proteins. *Annu Rev Genet* 1988;22:631–677. [PubMed: 2853609]
- Mahajan SD, Schwartz SA, Shanahan TC, Chawda RP, Nair MP. Morphine regulates gene expression of alpha- and beta-chemokines and their receptors on astroglial cells via the opioid mu receptor. *J Immunol* 2002;169:3589–3599. [PubMed: 12244149]
- Mahajan SD, Schwartz SA, Aalinkeel R, Chawda RP, Sykes DE, Nair MP. Morphine modulates chemokine gene regulation in normal human astrocytes. *Clin Immunol* 2005;115:323–332. [PubMed: 15893700]
- Mahajan SD, Hu Z, Reynolds JL, Aalinkeel R, Schwartz SA, Nair MP. Methamphetamine modulates gene expression patterns in monocyte derived mature dendritic cells: implications for HIV-1 pathogenesis. *Mol Diagn Ther* 2006;10:257–269. [PubMed: 16884330]

- Mailhos C, Howard MK, Latchman DS. Heat shock protects neuronal cells from programmed cell death by apoptosis. *Neuroscience* 1993;55:621–627. [PubMed: 8413925]
- Matsuda LA, Lolait SJ, Brownstein MJ, Young AC, Bonner TI. Structure of a cannabinoid receptor and functional expression of the cloned cDNA. *Nature* 1990;346:561–564. [PubMed: 2165569]
- McCarty MF. Down-regulation of microglial activation may represent a practical strategy for combating neurodegenerative disorders. *Med Hypotheses* 2006;67:251–269. [PubMed: 16513287]
- Morahan PS, Klykken PC, Smith SH, Harris LS, Munson AE. Effects of cannabinoids on host resistance to *Listeria monocytogenes* and herpes simplex virus. *Infect Immun* 1979;23:670–674. [PubMed: 313368]
- O’Gorman E, Beutner G, Wallimann T, Brdiczka D. Differential effects of creatine depletion on the regulation of enzyme activities and on creatine-stimulated mitochondrial respiration in skeletal muscle, heart, and brain. *Biochim Biophys Acta* 1996;1276:161–170. [PubMed: 8816948]
- Ogunro PS, Ogungbamigbe TO, Elemie PO, Egbewale BE, Adewole TA. Plasma selenium concentration and glutathione peroxidase activity in HIV-1/AIDS infected patients: a correlation with the disease progression. *Niger Postgrad Med J* 2006;13:1–5. [PubMed: 16633369]
- Pandey A, Mann M. Proteomics to study genes and genomes. *Nature* 2000;405:837–846. [PubMed: 10866210]
- Peterson PK, Sharp BM, Gekker G, Portoghese PS, Sannerud K, Balfour HH Jr. Morphine promotes the growth of HIV-1 in human peripheral blood mononuclear cell cocultures. *Aids* 1990;4:869–873. [PubMed: 2174676]
- Peterson PK, Gekker G, Hu S, Cabral G, Lokensgard JR. Cannabinoids and morphine differentially affect HIV-1 expression in CD4(+) lymphocyte and microglial cell cultures. *J Neuroimmunol* 2004;147:123–126. [PubMed: 14741442]
- Price TO, Ercal N, Nakaoke R, Banks WA. HIV-1 viral proteins gp120 and Tat induce oxidative stress in brain endothelial cells. *Brain Res* 2005;1045:57–63. [PubMed: 15910762]
- Pryce G, Ahmed Z, Hankey DJ, Jackson SJ, Croxford JL, Pocock JM, Ledent C, Petzold A, Thompson AJ, Giovannoni G, Cuzner ML, Baker D. Cannabinoids inhibit neurodegeneration in models of multiple sclerosis. *Brain* 2003;126:2191–2202. [PubMed: 12876144]
- Semenza GL, Jiang BH, Leung SW, Passantino R, Concordet JP, Maire P, Giallongo A. Hypoxia response elements in the aldolase A, enolase 1, and lactate dehydrogenase A gene promoters contain essential binding sites for hypoxia-inducible factor 1. *J Biol Chem* 1996;271:32529–32537. [PubMed: 8955077]
- Shannon P, Pennacchio LA, Houseweart MK, Minassian BA, Myers RM. Neuropathological changes in a mouse model of progressive myoclonus epilepsy: cystatin B deficiency and Unverricht-Lundborg disease. *J Neuropathol Exp Neurol* 2002;61:1085–1091. [PubMed: 12484571]
- Shen M, Thayer SA. Cannabinoid receptor agonists protect cultured rat hippocampal neurons from excitotoxicity. *Mol Pharmacol* 1998;54:459–462. [PubMed: 9730904]
- Smith AJ, Blumenfeld H, Behar KL, Rothman DL, Shulman RG, Hyder F. Cerebral energetics and spiking frequency: the neurophysiological basis of fMRI. *Proc Natl Acad Sci U S A* 2002;99:10765–10770. [PubMed: 12134056]
- Speth C, Prohaszka Z, Mair M, Stockl G, Zhu X, Jobstl B, Fust G, Dierich MP. A 60 kD heat-shock protein-like molecule interacts with the HIV transmembrane glycoprotein gp41. *Mol Immunol* 1999;36:619–628. [PubMed: 10499815]
- Tonella L, Walsh BJ, Sanchez JC, Ou K, Wilkins MR, Tyler M, Frutiger S, Gooley AA, Pescaru I, Appel RD, Yan JX, Bairoch A, Hoogland C, Morch FS, Hughes GJ, Williams KL, Hochstrasser DF. ‘98 *Escherichia coli* SWISS-2DPAGE database update. *Electrophoresis* 1998;19:1960–1971. [PubMed: 9740056]
- Tonge R, Shaw J, Middleton B, Rowlinson R, Rayner S, Young J, Pognan F, Hawkins E, Currie I, Davison M. Validation and development of fluorescence two-dimensional differential gel electrophoresis proteomics technology. *Proteomics* 2001;1:377–396. [PubMed: 11680884]
- Tusher VG, Tibshirani R, Chu G. Significance analysis of microarrays applied to the ionizing radiation response. *Proc Natl Acad Sci U S A* 2001;98:5116–5121. [PubMed: 11309499]
- Unlu M, Morgan ME, Minden JS. Difference gel electrophoresis: a single gel method for detecting changes in protein extracts. *Electrophoresis* 1997;18:2071–2077. [PubMed: 9420172]

- van der Stelt M, Di Marzo V. Cannabinoid receptors and their role in neuroprotection. *Neuromolecular Med* 2005;7:37–50. [PubMed: 16052037]
- van der Stelt M, Veldhuis WB, Bar PR, Veldink GA, Vliegthart JF, Nicolay K. Neuroprotection by Delta9-tetrahydrocannabinol, the main active compound in marijuana, against ouabain-induced in vivo excitotoxicity. *J Neurosci* 2001;21:6475–6479. [PubMed: 11517236]
- Wessel D, Flugge UI. A method for the quantitative recovery of protein in dilute solution in the presence of detergents and lipids. *Anal Biochem* 1984;138:141–143. [PubMed: 6731838]
- Wilm M, Shevchenko A, Houthaeve T, Breit S, Schweigerer L, Fotsis T, Mann M. Femtomole sequencing of proteins from polyacrylamide gels by nano-electrospray mass spectrometry. *Nature* 1996;379:466–469. [PubMed: 8559255]
- Zhou G, Li H, DeCamp D, Chen S, Shu H, Gong Y, Flaig M, Gillespie JW, Hu N, Taylor PR, Emmert-Buck MR, Liotta LA, Petricoin EF III, Zhao Y. 2D differential in-gel electrophoresis for the identification of esophageal scans cell cancer-specific protein markers. *Mol Cell Proteomics* 2002;1:117–124. [PubMed: 12096129]



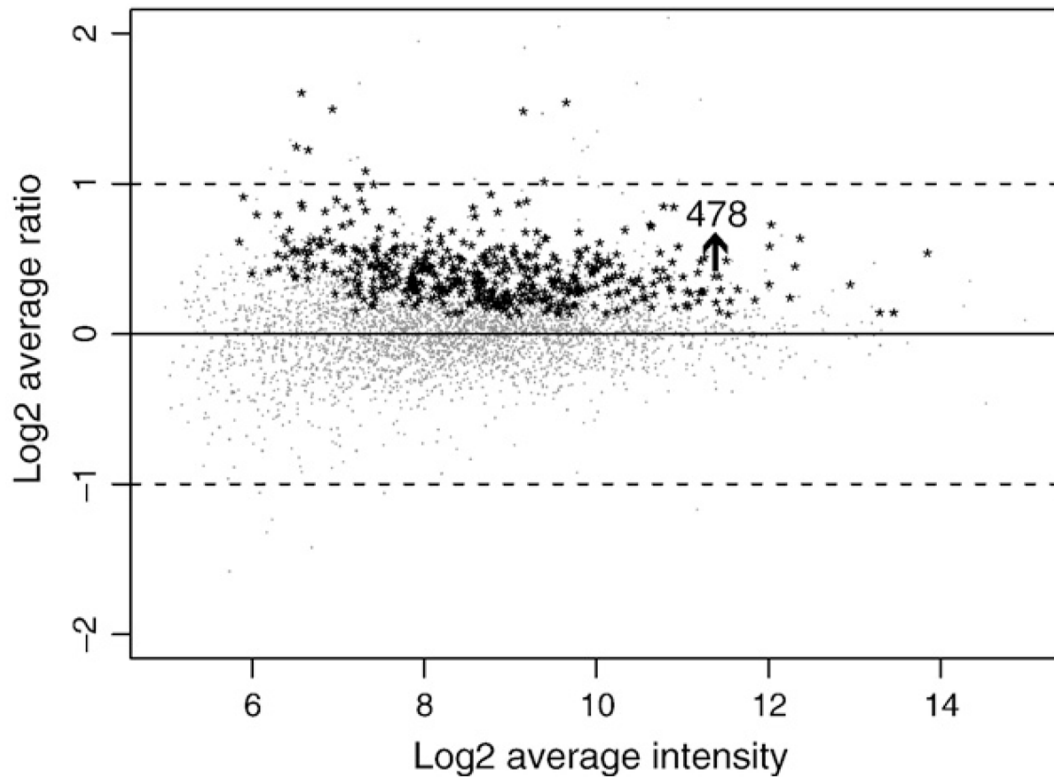


**Fig. 1.**

Scatter plot of total differentially expressed genes after treatment of NHA with  $\Delta^9$ -THC. NHA ( $1 \times 10^6$  cells/ml) were treated with  $10^{-7}$  M  $\Delta^9$ -THC for 48 hr. Total RNA was extracted from NHA and gene expression was determined by a microarray that focused on immunologically relevant genes. Statistically significant ( $p$  value  $< 0.05$ ), differentially expressed genes identified by two-step analysis of  $t$ -test and Significance Analysis of Microarrays (SAM) are shown as black asterisks (\*). All 478 differentially expressed genes were significantly up-regulated.

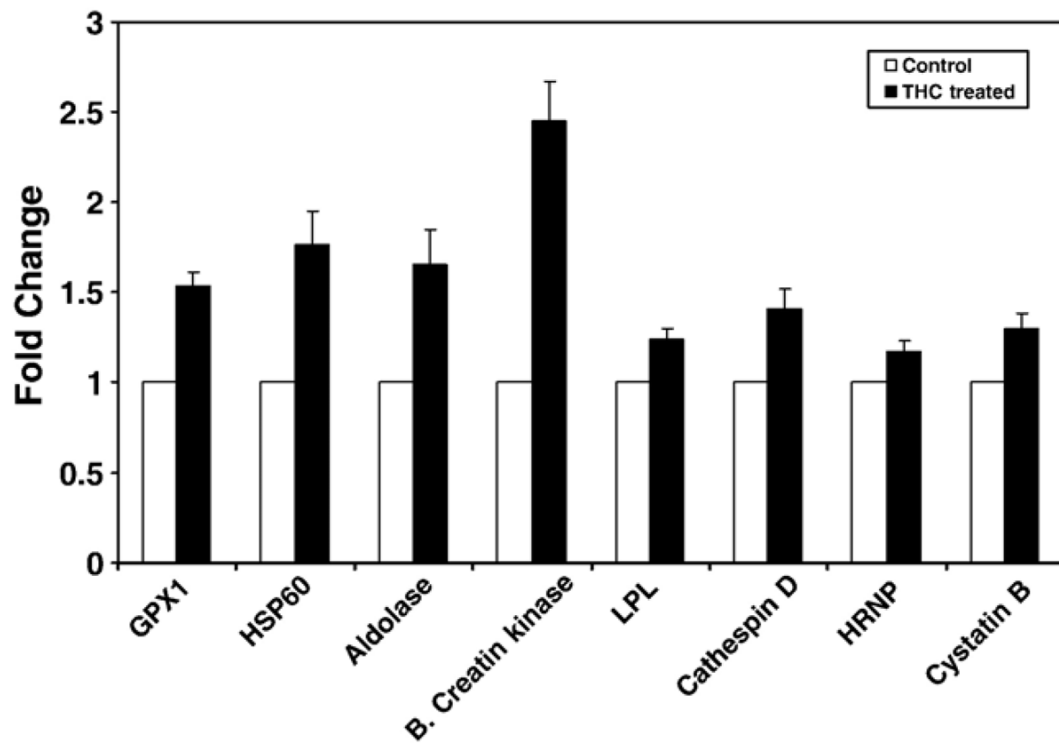


**Fig. 2.** Effect of THC on the up-regulation of specific genes as measured by Q PCR. NHA ( $1 \times 10^6$  cells/ml) were treated with  $10^{-7}$  M  $\Delta^9$ -THC for 48 h. Representative genes were selected for Q PCR analysis including glutathione peroxidase ( $p < 0.001$ ), HSP60 ( $p < 0.001$ ), aldolase A ( $p < 0.001$ ), brain creatine kinase ( $p < 0.001$ ), lysophospholipase 2 ( $p = 0.021$ ), cathepsin D ( $p = 0.011$ ), heterogeneous nuclear ribonucleoprotein F ( $p = 0.035$ ), and cystatin B ( $p = 0.018$ ). The results demonstrate that the expression of all selected genes was up-regulated upon treatment of NHA with  $\Delta^9$ -THC.

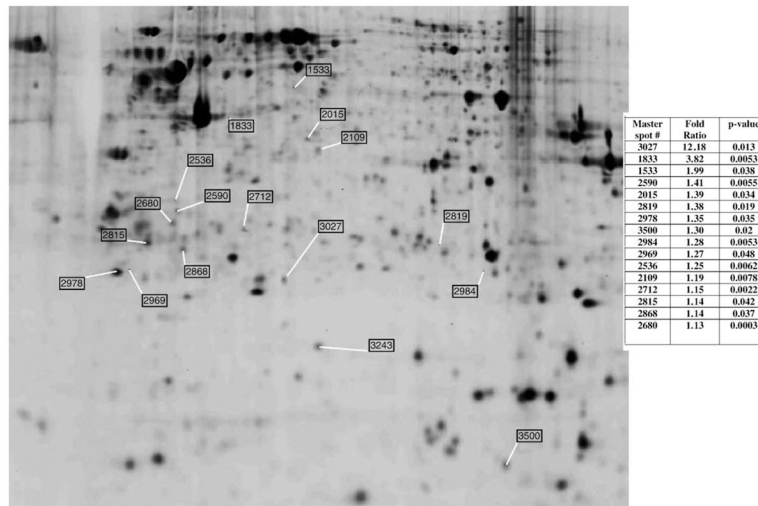


**Fig. 3.** 2D gel electrophoresis of proteins differentially expressed in response to treatment of NHA with  $\Delta^9$ -THC. NHA ( $1 \times 10^6$  cells/ml) were treated with  $10^{-7}$  M  $\Delta^9$ -THC for 48 h. Total protein was isolated, subjected to DIGE analysis, and stained with SYPRO Ruby protein gel stain as described in Experimental procedures. The pH increases from left to right and the molecular mass decreases from the top to the bottom of the gels. Identified protein spots are outlined and numbered. The table shows master spot numbers assigned during Decyder software analysis of gel images, fold-ratios of protein spots from THC treated and untreated samples and  $p$  values. Three separate experiments yielded similar results.

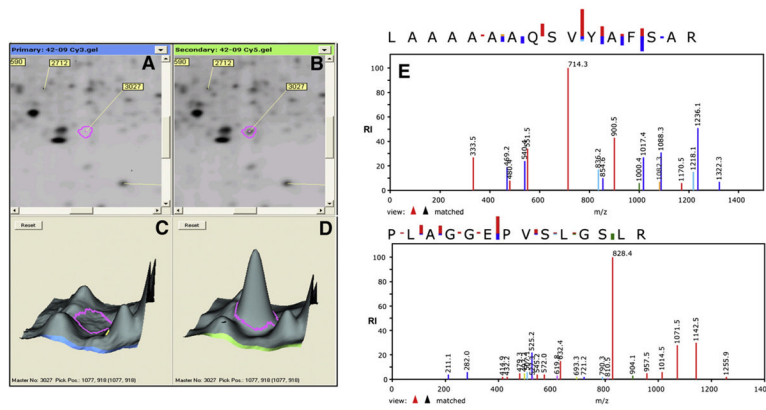


**Fig. 4.** Effect of  $\Delta^9$ -THC on differential protein expression by NHA. NHA ( $1 \times 10^6$  cells/ml) were treated with  $10^{-7}$  M  $\Delta^9$ -THC for 48 h. (A) 2D gel electrophoresis of untreated, control NHA. (B) 2D gel electrophoresis of  $\Delta^9$ -THC treated NHA. Spot #3027, representative of a gene whose expression was significantly up-regulated, was identified as glutathione peroxidase (GPX). (C) Protein abundance of GPX from untreated NHA. (D) Protein abundance of GPX from  $\Delta^9$ -THC treated NHA. (E) MS/MS spectra of fragment ions from 2 tryptic peptides, LAAAAAQS VYAFSAR and PLAGGEPVSLGSLR, obtained from spot # 3027 which was subsequently identified as glutathione peroxidase. These spectra represent the ion fragments that matched with the empirical database (noted as “view: ▲▲ matched” at the lower left of each spectrum).

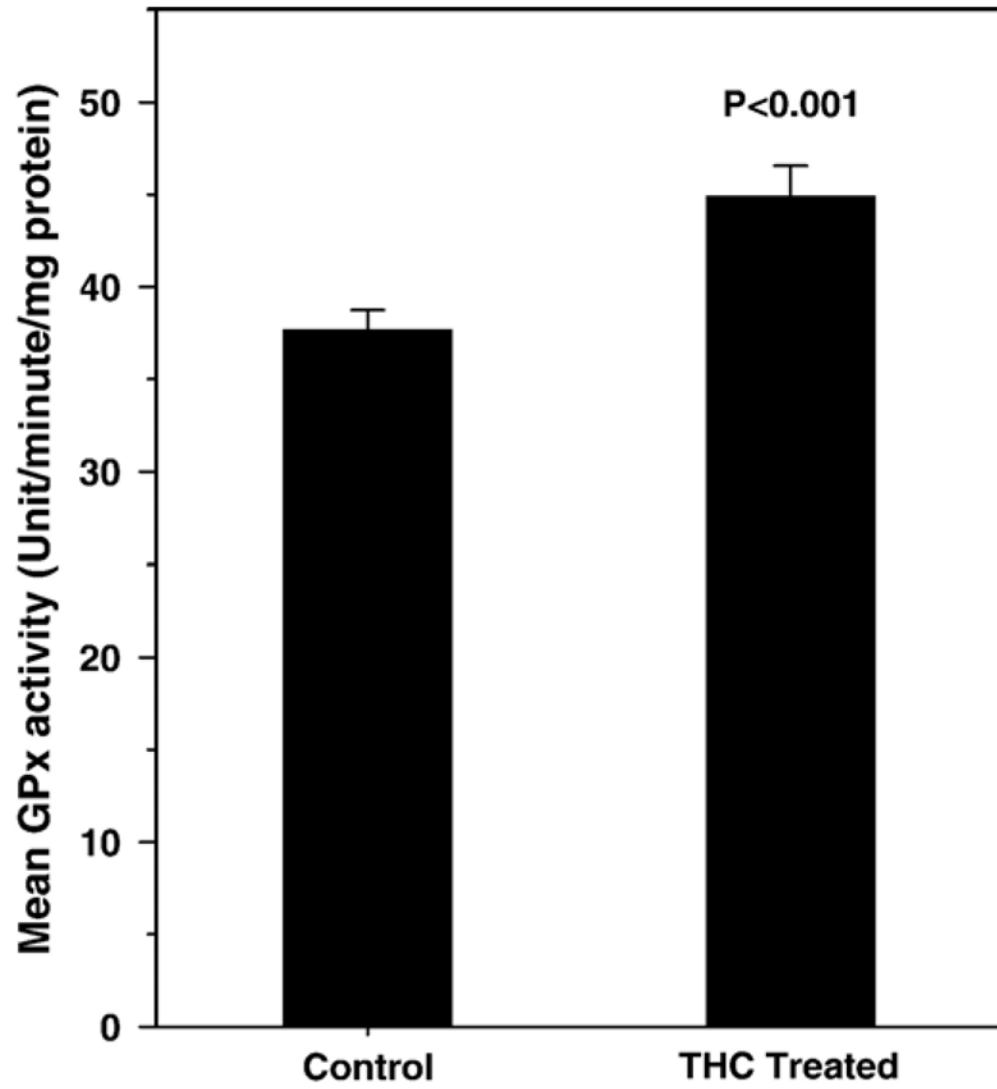


**Fig. 5.** Effect of  $\Delta^9$ THC on glutathione peroxidase production by NHA. NHA ( $1 \times 10^6$  cells/ml) were treated with  $10^{-7}$  M  $\Delta^9$ -THC for 48 h. Total protein was isolated and assayed for glutathione peroxidase activity.



**Table 1**Ontologic classification of genes significantly up-regulated in NHA treated with  $\Delta^9$ -THC

Functional categories	# of genes	p values
<i>Molecular functions</i>		
Phosphotransferase activity,	73	1.92E-06
Protein-tyrosine kinase activity	73	3.91E-06
Kinase activity	55	1.89E-05
Transcription regulator activity	54	3.14E-05
Protein kinase activity	41	0.0001159
GTPase activity	25	0.0006143
Protein serine/threonine kinase activity	24	0.0006753
GTP binding	24	0.0007858
Nucleoside-triphosphatase activity	24	0.0009844
Transferase activity	22	0.0011866
Protein kinase activity	15	0.0032568
Phosphoprotein phosphatase activity	14	0.0033315
CAMP-dependent protein kinase activity	12	0.0037705
Lyase activity	12	0.0042087
<i>Cellular processes</i>		
Cell proliferation	333	8.77E-12
Cell cycle	311	3.66E-11
Cellular process	230	2.54E-10
Regulation of cell cycle	122	1.81E-07
Cellular metabolism	115	1.87E-07
Mitotic cell cycle	110	4.09E-07
Metabolism	110	6.81E-07
Cellular macromolecule metabolism	73	4.00E-05
Protein kinase cascade	72	4.03E-05
Mitosis	43	8.10E-05
Regulation of apoptosis	43	8.70E-05
M phase of mitotic cell cycle	42	0.0001001
Response to stress	36	0.0001394
Cellular protein metabolism	27	0.0002379
Protein metabolism	23	0.000318
Cytokinesis	22	0.0004626
Intracellular signaling cascade	21	0.000795
Signal transduction	20	0.0008464

Gene expression was determined using microarrays. Gene ontology analysis of the microarray data was performed with GeneSifter™ software to classify significantly up-regulated genes into 2 categories: molecular functions and the cellular processes that they affect.

**Table 2**Modulation of gene expression by treatment of normal human astrocytes with  $\Delta^9$ -THC

ACC#	Fold-increase	Functional classification/gene nomenclature
		<i>Ubiquitin pathway</i>
R06895	2.79265	Ubiquitin specific protease 3
AI524284	1.85643	Cholinergic receptor, muscarinic 3
AA683308	1.84508	Protease, serine, 12 (neurotrypsin, motopsin)
AA158255	1.79570	Serine palmitoyltransferase, long chain base subunit 2
N33920	1.73270	Diubiquitin
AA425767	1.60745	Formyl peptide receptor 1
AA425211	1.60295	NADH dehydrogenase (ubiquinone)
		<i>Cell cycle regulation</i>
AA989185	1.64682	Cyclin K
AA598974	1.54597	Cell division cycle 2, G1 to S and G2 to M
AA009697	1.52337	Cell division cycle 42 (GTP-binding protein, 25 kDa)
		<i>Signal transduction regulation</i>
W45690	1.65368	Mitogen-activated protein kinase 1
AI381043	1.61382	Inositol 1,4,5-trisphosphate 3-kinase A
T67544	1.60163	Protein tyrosine phosphatase, receptor type, E
R26186	1.63948	Protein phosphatase 1, catalytic subunit, beta isoform
N63949	1.90466	Neurotrophic tyrosine kinase, receptor, type 2
R43753	1.52060	Alpha2,8-sialyltransferase
AA045508	1.54781	Adenylyl cyclase-associated protein 2
AA630320	1.58948	protease, serine, 15
		<i>Glucose metabolism</i>
AA424938	1.99451	Glucose-6-phosphate dehydrogenase
T53298	1.59825	Insulin-like growth factor binding protein 7
		<i>Transcriptional regulation</i>
N59534	1.88303	Ribosomal protein S15
		<i>Cytokines—pro- and anti-inflammation</i>
AA977194	1.50245	Interleukin 12 receptor, beta 2
H98636	1.63103	Tumor necrosis factor receptor superfamily, member 5
AI651871	1.52587	CD97 antigen (secretin receptor associated with inflammation)

NHA were cultured with and without  $10^{-7}$  M  $\Delta^9$ -THC for 48 h. Total RNA was isolated and used for microarray analysis. Gene expression was stratified based upon biological function. Data are presented as gene accession number (ACC#), functional classification and gene nomenclature, and significant fold-increase in expression in response to  $\Delta^9$ -THC treatment. Results are from 3 independent experiments using 3 different NHA cultures.

Methodological and biochemical details of statistically significant (Student's *t*-test), differentially expressed proteins after treatment of NHA with  $10^{-7}$  M  $\Delta^9$ -THC for 48 h

Table 3

Spot #	Protein name	GI No.	% sequence coverage	# of peptides matching/total peptides	Theoretical MW	Functions
3027	Glutathione peroxidase	gi 2144379	31	4/4	22.0	Anti-oxidant, protects hemoglobin in erythrocytes from oxidative breakdown
1833	Heterogeneous nuclear ribonucleoprotein F	gi 4826760	8.7	3/4	45.6	Protein binding
1833	Brain creatine kinase	gi 21536286	7.6	2/3	42.6	Creatine kinase activity
1833	Cathepsin D preproprotein	gi 4503143	5.8	2/2	44.5	Acid protease active in intracellular protein breakdown
1533	Putative elongation factor Tu	gi 11612420	4.3	1/2	23.2	Regulate transcription
1533	60 kDa heat shock protein	gi 129379	35	16/26	61.0	Molecular chaperon
2590	Enolase 1	gi 4503571	11	4/4	47.1	Phosphopyruvate hydratase activity/glycolysis
2015	Pyruvate kinase	gi 1363219	12	3/3	57.8	Protein binding/glycolysis
2015	Chloride intracellular channel 1	gi 14251209	16	2/2	26.9	Acts as a chloride ion channel
2819	Aldolase A	gi 229674	14	4/4	39.3	Glycolysis
2978	Tumor protein	gi 4507669	34	6/12	19.6	Calcium ion binding
2978	Chromobox homolog 1	gi 5803076	14	2/2	21.4	Chromatin binding/protein binding
3500	Cystatin B	gi 4503117	29	3/5	11.1	Endopeptidase inhibitor activity
2984	Lysophospholipase 2	gi 13786178	13	2/2	24.8	Protecting these cells from the cytolytic effects of the lysophospholipids
2969	Phosphoglycerate kinase 1	gi 4505763	10	3/5	44.6	ATP binding/phosphorylation
2969	Heat shock 70 kDa protein 5	gi 16507237	4.0	2/3	72.3	Nucleotide binding/protein folding
2536	Tubulin alpha 6	gi 14389309	9.6	3/3	49.9	Protein binding
2109	Glyceraldehyde-3-phosphate dehydrogenase	gi 7669492	8.7	2/2	36.0	Glycolysis
2712	Prohibitin	gi 4505773	31	10/23	29.8	Inhibits DNA synthesis
2712	Ribosomal protein S4	gi 4506725	9.1	2/2	29.6	Exoribonuclease activity/protein binding
2815	Rho GDP dissociation inhibitor	gi 4757768	35	10/23	23.2	Anti-apoptosis/negative regulation of cell adhesion
2815	Tumor protein D54 (hD54)	gi 20141658	14	2/2	22.2	Cell proliferation/protein binding
2868	RAN binding protein 1	gi 4506407	27	6/8	23.3	Regulation of translation
2680	Porin 31HM	gi 238427	17	4/7	30.6	Apoptogenic/anion transport

Proteins were subjected to DIGE analysis and identified by HPLC-MS/MS as described in Experimental procedures. Data include protein name, gene accession number (GI No.), % sequence coverage of the identified peptide, number of matching peptides, theoretical mass, and the known functions of the identified protein. Results are from 3 independent experiments using 3 different NHA cultures.